Biochimica et Biophysica Acta, 772 (1984) 273–287
Elsevier

BBA 72094

STUDIES OF THE KINETICS OF Na^+ GRADIENT-COUPLED GLUCOSE TRANSPORT AS FOUND IN BRUSH-BORDER MEMBRANE VESICLES FROM RABBIT JEJUNUM

FREDERICK C. DORANDO and ROBERT K. CRANE

University of Medicine and Dentistry of New Jersey Rutgers Medical School, Department of Physiology and Biophysics, Piscataway, NJ 08854 (U.S.A.)

(Received December 8th, 1983)

Key words: Glucose transport; Na^+ dependence; Kinetics; Brush-border membrane; (Rabbit intestine)

The Na^+-dependent D-glucose transport reaction in rabbit jejunal brush-border vesicles was studied. Initial rate data were obtained by fitting a polynomial equation to progress curves at different D-glucose concentrations and extracting the slope of the tangent at zero-time. Kinetic replots of the initial rate values produced biphasic Hofstee patterns indicative of two pathways for transport distinguished by their K_m values for glucose. Neither was dependent on the presence of a membrane potential. Both were dependent on Na^+ and both were inhibited by phlorizin. Increasing external sodium was found to elevate the apparent V_{max} for both pathways. Internal sodium was inhibitory. Pulsed progress curve analysis indicated that the effect of internal sodium was best characterized as carrier sequestration by a sodium-carrier binary complex. Inhibition by internal sodium was completely reversed by the presence, internally, of D-glucose. The presence of two pathways and the kinetic constants for these pathways do not agree with the conclusions of Hopfer and Groseclose (1980) J. Biol. Chem. 255, 4453–4462). Experiments are presented which bear on the reason for the disagreement.

Introduction

The kinetics of Na^+ gradient-coupled D-glucose transport in rabbit jejunal brush-border membrane vesicles have been reported by Hopfer and Groseclose [1] to be those of a single system following an ordered bi-bi mechanism with glide symmetry, adding Na^+ first from the outside. The studies were carried out for the most part by equilibrium exchange measurements under conditions in which there were no imposed transmembrane gradients of ions or glucose and no membrane diffusion potential. While acknowledging the validity of this approach for a study of kinetics, one may nonetheless emphasize that the question was not addressed whether the same or a modified kinetic mechanism obtains under the influence of imposed gradients and a membrane diffusion potential; that is, under conditions which are normal for the membrane of the living, active cell, in situ. It has been pointed out by others [2] that the data of Hopfer and Groseclose, though they seem to reasonably fit a single system with an ordered bi-bi mechanism, fail to specifically exclude randomness; that is, multiple pathways to the central complex, in some portion of the overall mechanism. This failure was acknowledged by the authors. However, Hopfer and Groseclose also failed to test for the presence of multiple systems. Data in the literature support the presence of two pathways or two systems for glucose transport in the intact intestine of the rat [3] and the hamster [4] studied in vitro.

Over a period of years, we have carried out

kinetic studies using vesicles taken from the same source; rabbit jejunal brush-border membrane, and prepared by substantially the same calcium precipitation method [5]. We have used a wide variety of gradient conditions in addition to equilibrium exchange conditions and we have studied the system with respect to the effects of glucose and Na^+ concentrations inside the vesicles as well as out. We have taken into account insofar as possible the objections of Hopfer [6–9] to studies of transport in vesicles under gradient conditions. We have paid particular attention to the possible influence on the results of membrane depolarization due to solute-coupled Na^+ flux and of heterogeneity in the vesicle population. As will be seen, neither one is an important hindrance in the study of kinetics. Our findings show the presence of two pathways for glucose transport which, at the present state of experimentation, appear most likely to represent two individual transport systems. In addition, there are strong experimental arguments indicating that Hopfer and Groseclose mixed the kinetic properties of these two pathways in arriving at their conclusions. Direct experimental tests of the predictions of the Hopfer model with regard to the effects of internal Na^+ and glucose fail to support it.

Materials and Methods

Vesicle preparation. Vesiculated jejunal brush-border membranes from male New Zealand white rabbits were obtained by a modification of the method of Malathi et al. (1979) [5]. After the first $27000 \times g$ spin the membranes were resuspended in a 5 mM Hepes-Tris (pH 7.5) loading solution containing mannitol or salts, as specified in the legends to the various figures for the internal constituents. After 15 min at 25°C the vesicle suspension was were spun down at $3000 \times g$ at 4°C, the pellet discarded and the supernatant was spun at $27000 \times g$ for 30 min at 4°C. This final pellet was resuspended in the loading solution at 4°C to a final concentration of approx. 15 mg protein/ml and allowed to equilibrate an additional 30 min. When valinomycin was required, an ethanolic solution was placed in the tube and dried under a stream of nitrogen prior to vesicle addition to a final value of approx. 1 μg per mg protein. This procedure was later modified by adding a 100 μl aliquot of the loading solution to the valinomycin tube followed by a 5 s sonication on a bath sonicator to disperse the ionophore. The described manipulation of the membrane potential was accomplished by utilizing K^+ concentrations which ensured a high fractional saturation of valinomycin [10]. The vesicles were not stored for later use. The entire procedure was performed on the day of the experiment using two or more rabbits, and was always completed within 3.5 h of the sacrifice. The assays were performed immediately following vesicle preparation.

Sodium equilibrated vesicles. The vesicles were prepared as described above with the following modifications. The first $27000 \times g$ pellet was divided into two parts for different loading procedures. One part was resuspended with 100 mM mannitol, 5 mM Hepes-Tris (pH 7.5), and the other part was resuspended with 100 mM NaSCN, 100 mM mannitol, 5 mM Hepes-Tris (pH 7.5). All ensuing steps were identical. Vesicles were spun down at $27000 \times g$ for 20 min at 4°C. The resulting pellets were resuspended in 100 mM NaSCN, 100 mM mannitol, 5 mM Hepes-Tris (pH 7.5), and gramicidin (approx. 1 μg/mg protein). The vesicles were allowed to equilibrate in this medium for 30 min at 21°C, and then placed on ice and assayed for D-glucose uptake at 15°C by the technique described below.

Incubation and assay. Each incubation tube received a maximum of three different additions: (1) a cocktail containing all the constant materials including the radiolabeled compound, (2) unlabeled sugar, and (3) water to a final volume. The cocktail volume prepared was sufficient for addition to all tubes comprising a single kinetic curve.

The reaction in each tube was initiated with the addition of 50 μl of ice-cold vesicles by a Rainin pipetman. Rapid and thorough mixing was assured by discharging the vesicles directly into the reaction mixture, and then flushing the tip with the reaction fluid twice. The uptake was stopped at the time indicated by the addition of 1 ml of ice-cold fluid of the same composition as the reaction medium without D-glucose. The mixture was vortexed and rapidly passed through the central

portion of a 0.45 μm HAWP millipore filter and immediately washed with 3 ml of the same ice-cold stopping solution. The filter was placed in a vial containing scintillation fluid plus methyl-cellosolve, allowed to dissolve overnight and counted to a accuracy of ±1% in a Beckman LS200. Preparation and execution of the assay in this manner was found to have a precision of ±2%. The protein was determined by the method of Lowry et al. [11]. All short time assays were completed within approx. 90 min. The assay tubes designated to measure space were always begun prior to the short time assays, and ended between 90 and 120 min later. Space determinations were always done in duplicate on every curve. All subsequent calculations are as described.

3-s Pulse assay. The 3-s pulse assay was carried out in two stages. First a progress of reaction curve was created with labeled D-glucose by preparing multiple identical assay tubes (300 μl) to which 50 μl of vesicles were added at time zero, and the reaction terminated at various times according to the same procedure for the kinetic assays. The second part of the test was carried out by preparing multiple identical assay tubes (300 μl) containing unlabeled D-glucose. The reaction was initiated by the addition of 50 μl of vesicles and allowed to proceed. At selected intervals a 200 μl volume of identical medium composition containing labeled D-glucose was added and terminated after 3 s in the manner described above.

Calculations. Curves resulting from multiple determinations were averaged at each substrate concentration. Uptakes were converted to internal concentration by dividing by the internal volume per mg protein. progress curves were analyzed by fitting a polynominal in time [12] with the NLIN procedure available from the Statistical Analysis Service Institute, Cary, NC. The resulting zero-time rate, expressed as V in the Hofstee plots, has the units of internal sugar concentration per min unless otherwise noted in the legend. Biphasic Hofstee plots were analyzed as the sum of two Michaelis-Menten functions by the same package procedure.

The D-glucose uptake in Fig. 14 was measured at 0.1 min and corrected to the zero-time rate according to the integrated rate equation for a diffusion process (i.e., $[P] = [S] \cdot (1 - e^{-kt})$) and the non-mediated diffusion component was subtracted.

Materials. All reagents were obtained from commercial sources and were of the highest purity available; mannitol, Tris base, Hepes, phlorizin from Sigma Chemical Co., sodium sulfate from Fisher Scientific Co.; sodium chloride and potassium chloride from Mallinckrodt; potassium sulfate from Matheson, Coleman and Bell; sodium thiocyanate from J.T. Baker.

D-[U-^{14}C]Glucose (316 mCi/mmol) was purchased from Amersham/Searle Co. L-[U-^{3}H]Glucose (17.46 Ci/mmol) and 3-*O*-methyl-D-[U-^{14}C]glucose (347 mCi/mmol) were purchased from New England Nuclear Corp. Radioactive ^{22}Na was purchased from Amersham as the carrier free radionuclide.

Methyl-cellosolve was purchased from national Diagnostics.

Results

Vesicle population

It is known that the vesicle preparation used in these and many other studies is not morphologically homogeneous. Although the preparation is predominantly composed of vesicles showing a 'normal' distribution about a mean diameter of 135 nm (Fig. 1), it does contain significant amounts of other forms (see legend to Fig. 1). It was our concern that the vesicle preparation act in a relatively homogeneous manner with respect to certain key functional parameters.

Since the different morphological forms sediment at different rates under the influence of centrifugal force, we chose to use incremental centrifugation to achieve preparations differing widely in their content of the different forms and then to examine their transport characteristics. Three fractions were retrieved at the g forces listed in Table I and examined under the electron microscope. The lowest g spin contained large vesicles, multilaminar vesicles and cellular debris. This fraction, morphologically the most complex and routinely removed during the preparation of vesicles as described above, might be expected to differ substantially in its activities from the other

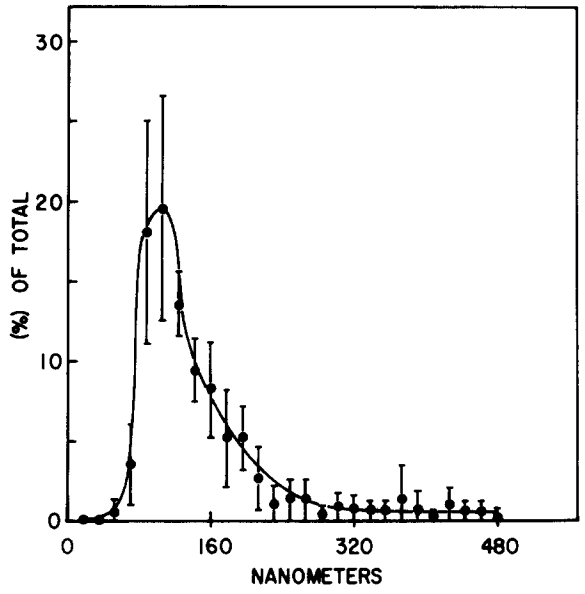

Fig. 1. The distribution of vesicle sizes in a preparation made from rabbit jejunal brush-border membranes. The vesicle preparation was composed at 67% round vesicles (see Figure), 28% tubular forms (0.16 μm×0.8μm), 3.3% large vesicles (0.8 μm) 1.7% multi-vesicular forms. To determine the distribution, electron micrographs were taken at 5000× magnification. 15–25 micrographs were taken at random and projected on the screen of a stereology counting device after 5-fold magnification. 1000–2000 structures were counted from several micrographs. Three different procedures varying fixation and staining gave the same distribution.

fractions. However, the data in Table I and Fig. 2 show that its transport functions are closely similar to those of the higher g material, fractions 2 and 3. The intermediate g spin, fraction 2, contained mostly round vesicles with a mean diameter of 135 nm. The highest g spin, fraction 3, containing mostly tubular forms with a short axis matching the diameter of the vesicles in fraction 2 and a variable long axis up to approx. 800 nm. These tubular forms presumably represent microvilli that are in various degrees of conversion into round vesicles. Fractions 2 and 3 are functionally indistinguishable (Table I, Fig. 2).

It seems reasonable to conclude that the kinetic features of transport to be described herein, including the curvilinear nature of the Hofstee plot (Fig. 2), reflect properties of the membrane carriers. Any contribution to these by the morphology of the membranous elements is beyond the limits of sensitivity of the methods used.

TABLE I

D-GLUCOSE MEASURED VESICLE PARAMETERS

The vesicle parameters are determined under 300 mM mannitol equilibrium.

Fraction	Force (g)	Total space (μl/mg)	Dead space (μl/mg)	Diffusion (min^{-1})	% Total protein
1	3000	0.64	0.052	0.25	10.6
2	12000	0.70	0.035	0.27	69.7
3	27000	0.80	0.049	0.27	19.8

Diffusion

The entry of D-glucose into brush-border membrane vesicles under non-energized (sodium-free) conditions appears to represent a simple situation where a substrate is diffusing across a semi-permeable barrier into a space until its concentration across the barrier is equal. As compared to cellular systems where metabolism may occur, vesicular

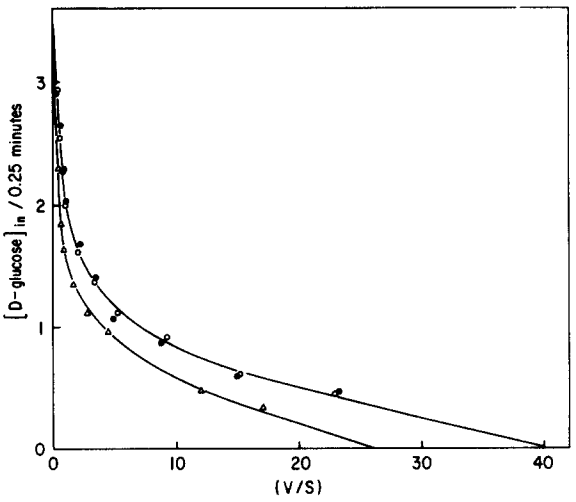

Fig. 2. Vesicle D-glucose transport capacity. Vesicles were loaded with 300 mM mannitol/5 mM Hepes-Tris (pH 7.5). The reaction was initiated by the addition of 50 μl of vesicles to a 300 μl cocktail yielding a final composition of 100 mM Na_2SO_4, 5 mM Hepes-Tris pH 7.5, 43 mM mannitol 20 μM D-[^{14}C]glucose, and unlabeled D-glucose up to 8 mM. The reaction was terminated at 0.25 min. Vesicles were pellets at $3 \cdot 10^3$ g (△), $12 \cdot 10^3$ g (●), and $27 \cdot 10^3$ g (○).

TABLE II

VESICLE CHARACTERISTICS UNDER IONIC CONDITIONS

The vesicles contain valinomycin at 1 μg/mg protein.

Experimental conditions medium/vesicles	*N*	Total space (μl/mg protein)	Diffusion constant (min^{-1})	Dead space (μl/mg protein)
1. 250 mM K_2SO_4/250 mM K_2SO_4	6	0.82 ± 0.06	0.38 ± 0.05	0.039 ± 0.005
2. 300 mM mannitol/100 mM K_2SO_4	10	0.82 ± 0.13	0.24 ± 0.09	0.035 ± 0.01
3. 1 M mannitol + 0.5 M KCl/ 1 M mannitol + 0.5 M KCl	10	0.92 ± 0.11	0.17 ± 0.07	0.028 ± 0.01
4. 0.15 M mannitol + 0.25 M K_2SO_4 0.15 M mannitol + 0.25 M K_2SO_4	10	0.72 ± 0.09	0.28 ± 0.07	0.021 ± 0.005

systems are indeed simple. However, even in vesicular systems, where no metabolism of substrate occurs [13], this simple diffusion process can be complicated by four background reactions: (a) an external binding reaction, (b) an internal binding reaction, (c) a facilitated entry, and (d) a non-specific, non-saturable trapping of substrate at zero time in a 'dead space'. If the principle reaction that occurs is diffusion, then the relative contribution of these four backgrounds can be determined.

Of these background reactions the dead space is the simplest to measure, and represents a correction to be applied to all the uptake data. The correction is simply a subtraction of the amount of label which can not be removed from the filters (with vesicles) at time zero. However, care was taken to distinguish between this quantity and a contribution made to it by an external binding reaction. This was accomplished by adding a 100- to 1000-fold excess of the unlabeled substrate thereby substantially reducing the amount of labeled substrate specifically bound or available for transport. The actual measurement of the dead space and the diffusion constant parameters reported in Tables I and II was carried out by following the uptake of 20 μM D-[^{14}C]glucose to which 8 mM unlabeled D-glucose had been added over the time period from 3 s to 15 s, and at 90 min. The 90-min equilibrium value was taken as a measure of the total space, converted into μl per mg protein, and then used to convert the short-time uptake values into internal concentrations. The internal concentration versus time curve was completely linear up to 15 s and yielded a finite value at zero time. That value represents the dead space, and is expressed as μl per mg protein in Tables I and II. The slope of the line represents the initial rate of diffusion at 8020 μM D-glucose, and the diffusion constant (k) can be extracted according to the following equation for simple diffusion.

$$\frac{d[P]}{dt} = k \cdot ([S] - [P]) \quad (1)$$

The zero-time rate constants listed in Tables I and II agree with the half-times for diffusion reported by Hopfer and Groseclose [1].

Two secondary considerations which could complicate kinetic data were envisioned: (1) alterations in equilibrium space due to the imposition of salt gradients, and (2) alterations in the functional space at short times when kinetic assays were performed under gradient conditions. The data in Tables I and II indicate that these problems do not exist here. The functional space remained the same with and without the potassium salt gradient and was not different from the mannitol space. The initial rate of diffusion was computed from those functional space values and was equally unaltered. If the short-time internal volume had increased significantly, then the diffusion rate would have increased as a consequence of the large internal volume.

The determination of external binding was assessed in an analogous manner by creating a progress curve over the first 0.8 min interval using a 20 μM concentration of undiluted label and de-

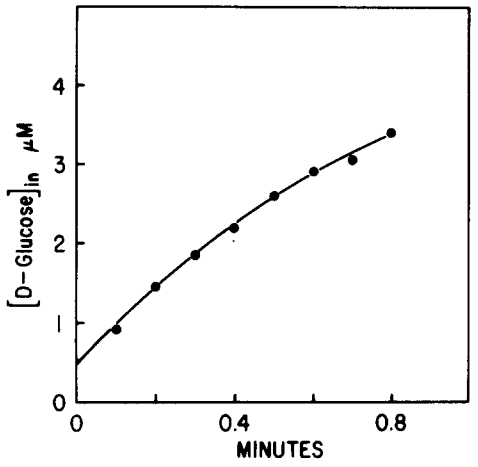

Fig. 3. Sodium free D-glucose uptake. Vesicles were as described in Fig. 1, and the reaction was initiated by the addition of 50 μl of vesicles to a 300 μl cocktail yielding a final medium composition of 300 mM mannitol, 5 mM Hepes-Tris (pH 7.5), and 20 μM D-[^{14}C]glucose. ($N = 12$) Equation $P = a + bt + ct^2$.

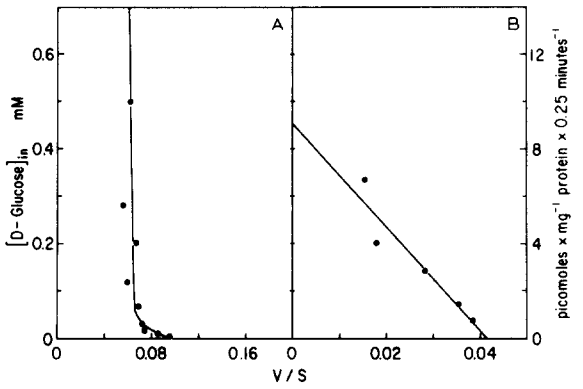

Fig. 4. Hofstee plot of D-glucose binding at 0.25 min. All conditions are the same as those described in Fig. 2, except a variable D-glucose concentration was achieved by the addition of unlabeled sugar up to 5 mM. ($N = 18$).

termining the internal concentration on the basis of the equilibrium space measured at 90 min (Fig. 3). Computer analysis of the curve by polynomial fitting [12] gave a zero-time intercept of 0.43 pmol/mg protein and a diffusion of 0.27 min^{-1}. The value for diffusion agrees with that found at high ratios of unlabeled to labeled substrate (Tables I and II). The intercept value presumably represents external binding of the D-glucose substrate. To test this idea, we constructed a Hofstee plot (Fig. 4) at 15 s to take advantage of the fact that facilitated entry is a time-dependent process. Then, by extracting a K_m and V_{max} for the process the amount of binding that would be present at 20 μM D-glucose was approximated. The curve in Fig. 4 was resolved into $K_m = 145$ μM; $V_{max} = 8.9$ pmol/mg protein and a vertical, diffusion component ($k = 0.23$ min^{-1}). Diffusion was in the same range as before. The 15 s binding at 20 μM D-glucose was calculated to be 1.0 pmol/mg protein which agrees with the zero-time intercept above within the limits of sensitivity of the methods used.

Two additional sugars, 3-*O*-methyl-D-glucose and L-glucose, were assessed for binding (V_{max}) in the same manner as for D-glucose in Fig. 4. 3-*O*-Methyl-D-glucose showed 5 pmol/mg protein of binding with a K_d in the range of 300 μM, while L-glucose did not show any measurable binding. This result is consistent with the relative K_m values of these sugars for uptake in the presence of Na^+. 3-*O*-Methyl glucose has a higher K_m than D-glucose [4], and L-glucose has an exceedingly poor relative K_m [14], at least in the hamster. The number of glucose binding sites found in the Na^+-free condition is about the same, within the limits of error, as the number of Na^+-dependent, D-glucose protectable, high affinity phlorizin binding sites (13.5 pmol/mg protein) reported by Toggenburger et al. [15].

Internal binding was examined by measuring the displacement of the equilibrium functional space from the value obtained at high unlabeled to labeled ratios * of D-glucose versus substantially lower ratios at 90 min. No additional binding could be detected (data not shown).

Initial rates under Na^+-gradient conditions

In order to have data that can be used to define a probable kinetic mechanism two experimental conditions must be fulfilled; a wide range (2–3 orders of magnitude) of concentrations for both substrates must be examined and the data obtained from measurements in real time must be

* Total space = Functional space and Dead space. Dead space represents a trapping of label on the filter with vesicles present that can not be removed by high concentrations of unlabeled substrate.

corrected to time zero. The latter condition is particularly important for the vesicular system under gradient conditions. It is well appreciated that gradient conditions established at the beginning of incubation decay substantially within the first minute. It is, perhaps, not so well appreciated that diffusion may also be complex as when gradient conditions are selected that produce an 'overshoot'. Overshoot is an uptake of D-glucose into the vesicles to a concentration that exceeds that in the external medium. As uptake proceeds net diffusion is, at first, inward. As the internal concentration equals and then surpasses the external, net diffusion reverses direction. Overshoot is observed throughout the micromolar range for D-glucose, at 20 μM it can attain a nearly 100-fold gradient, in/out, on a time scale of seconds. Uptake rates measured in real time are thus underestimated not only because of the expected back reaction but also because of back diffusion. This problem disappears in the low millimolar range of glucose concentration because the degree of overshoot greatly diminishes. Above about 5 mM glucose the degree of overshoot is below the limit of experimental detection. Diffusion is an important correction only at longer times and/or when overshoot is very high. However, the entire problem is

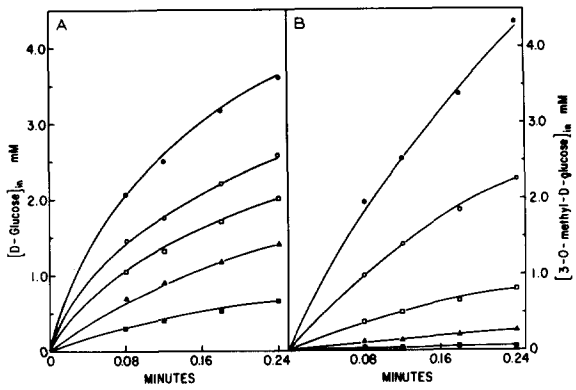

Fig. 5. Progress of reaction. Vesicles were loaded with 200 mM mannitol, 5 mM Hepes-Tris (pH 7.5). The reaction was initiated by the addition of 50 μl of vesicles to a 300 μl cocktail yielding a final medium composition of 100 mM NaSCN, 5 mM Hepes-Tris (pH 7.5), 28 mM mannitol, and sugar. (A) D-Glucose medium concentrations are: ■, 20 μM; △, 100 μM; □, 420 μM; ○, 2020 μM; ●, 8020 μM. ($N = 12$). (B) 3-*O*-Methyl-D-glucose concentrations ($N = 1$). The symbols indicate the same concentrations as in (A).

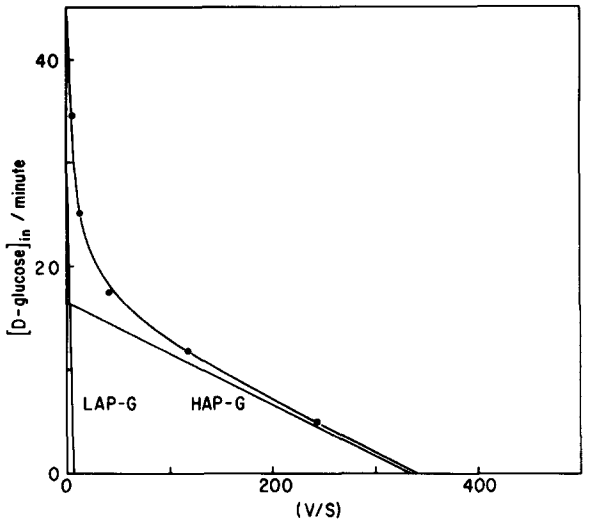

Fig. 6. Computer generated initial rates. A replot of the initial rates at zero time minus inward diffusion derived from the D-glucose progress curves in Fig. 4A. HAP-G, pathway of relatively high affinity for glucose; LAP-G, pathway of relatively low affinity for glucose.

circumvented by extrapolation of real time data to time zero, as is done in the experiments reported herein. Diffusion correction is then made simply by direct subtraction of the initial rate diffusion component ($k \cdot [S]$) from the total rate.

The correction to initial rate can be carried out in either of two ways: (1) by fitting an integrated rate equation which describes the forward reaction rate and the parameters contributing to its decay over time, or (2) by fitting Equation 2 which is a

$$[P] = \beta_1 \cdot t + \beta_2 \cdot t^2 + \ldots \quad (2)$$

polynomial in time that describes the shape of the curve while ignoring the relationship between the physical parameters that generate that shape [12]. Because we wanted to make no assumptions about the nature of the transport reaction or its kinetics we used the latter method. Typical progress curves are shown in Fig. 5. The D-glucose values for β_1 minus the diffusion component derived from Fig. 5 were replotted in Hofstee form (Fig. 6) and the kinetic constants were extracted as described in Materials and Methods (Table III).

There are two pathways shown in Fig. 6, one of relatively high affinity for D-glucose (HAP-G) and

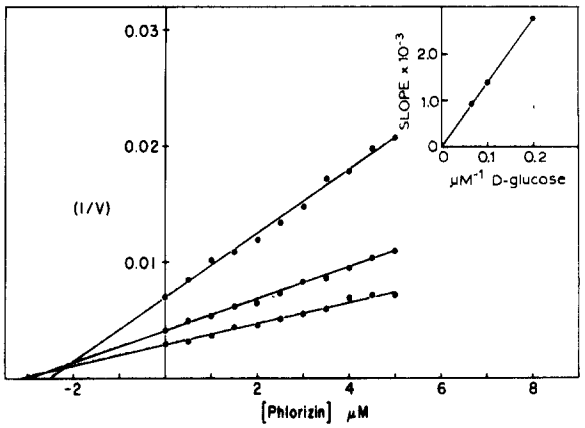

Fig. 7. Dixon plot of phlorizin inhibition at 0.25 min. Vesicles were loaded with 200 mM mannitol and 5 mM Hepes-Tris (pH 7.5). Reaction was initiated by the addition of 50 μl of vesicles to a 300 μl cocktail yielding a final medium composition of 100 mM NaSCN, 5 mM Hepes-Tris (pH 7.5), 29 mM mannitol. The concentration of D-[^{14}C]glucose was 5 μM, 10 μM, and 15 μM. The inset is a primary slope replot of the slopes for the three curves (Segel [16]). ($N = 5$).

the other of relatively low affinity (LAP-G). Except when the [Na^+] is severely restricted [16], biphasic curves are obtained in plots of corrected or uncorrected data at any time coordinate as in Fig. 6. The principle effect of extrapolating the data to $t = 0$ is to elevate the apparent V_{max} parameter in both legs of the biphasic curve. The apparent K_m values, which appear to shift upward with data correction, are actually rather stable within the limits of confidence.

To further characterize the two pathways, the classic inhibitor of the Na^+-dependent D-glucose transport reaction, phlorizin, was tested for inhibition across the entire D-glucose concentration range, 5 μM to 8020 μM. The data are displayed in two Dixon plots, Figs. 7 and 8, because of the different ranges of phlorizin which were needed to inhibit the two pathways. Under conditions of a 100 mM NaSCN gradient D-glucose was tested from 5 μM to 15 μM which in effect isolated the inhibition to the HAP-G pathway because the relative contribution to the velocity from the LAP-G pathway is less than 2% due to the wide difference in apparent K_m values (Fig. 7). The inhibition by phlorizin was the usual high affinity type ($K_i = 2.25$ μM ± 0.3) reported by other laboratories [13,15,17], and the primary slope replot (inset)

TABLE III

KINETIC PARAMETERS FOR Fig. 6

Apparent process	Apparent K_m (mM)	Apparent V_{max} (mmol/min)
LAP-G	4.1 ±1.7	27.5±2.8
HAP-G	0.049±0.013	16.6±1.76

shows the inhibition to be of the 'pure competitive' type. The data in Fig. 8 display the D-glucose concentration range from 420 μM to 8020 μM under conditions of a 100 mM Na_2SO_4 gradient. The intersection points in the second quadrant, which denote the apparent inhibition constant on the x-axis, actually progress from a low value of approx. 50 μM to a high value of approx. 120 μM. The relatively smooth progression of the intersection points is consistent with the interpretation that as the D-glucose concentration is increased and more of the LAP-G pathway is contributing to the velocity the inhibition constant is shifting upwards to reflect an averaging of two inhibitions

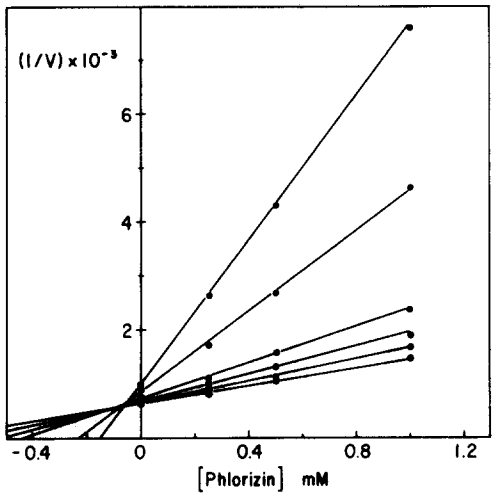

Fig. 8. Dixon plot of phlorizin inhibition at 0.25 min. Vesicles were loaded with 300 mM mannitol and 5 mM Hepes-Tris (pH 7.5). Reaction was initiated by the addition of 50 μl of vesicles to a 300 μl cocktail yielding a final medium composition of 100 mM Na_2SO_4, 5 mM Hepes-Tris (pH 7.5), 43 mM mannitol, 20 μM D-[^{14}C]glucose plus unlabeled D-glucose yielding final concentrations of 420, 820, 2020, 3020, 5020 and 8020 μM. Each curve represents a single D-glucose concentration. ($N = 4$).

corresponding to the two uptake pathways previously demonstrated.

It is difficult to assign a value to the inhibition constant for the LAP-G pathway, except to say that it is greater than or equal to 120 μM. A primary slope replot (not shown) of the combined inhibitions in Fig. 8 leads to a pure competitive result. The resulting ratio for the D-glucose K_m values in the two pathways (i.e., LAP-G/HAP-G $\cong$ 80) is mimicked by the phlorizin K_i values (i.e., LAP-Phl/HAP-Phl $\cong$ 50). This result is significant for several reasons; namely, (1) Hopfer and Groseclose found only one K_i for inhibition by phlorizin, and (2) their K_i value for inhibition more closely resembles the K_i we find for HAP-G, while their K_m value for D-glucose resembles the value we find for LAP-G. The apparent discrepancy in the number of pathways and in the pathway mismatch for the inhibition constant suggest that the transport process(es) found in these brush-border membrane vesicles may not be completely described by the model put forth by Hopfer and Groseclose [1]. These discrepancies are examined in more detail in a later section.

Experimental rate analysis of the progress curves

Overshoot has been characterized many times in time curves of Na^+ gradient-coupled D-glucose transport into brush-border membrane vesicles (e.g., Refs. 15, 17–20). Invariably, the shape of the overshoot curve has been ascribed to the response of transport to the electrochemical Na^+ gradient as it is initially imposed and then decays with time (e.g., Ref. 21). This explanation is satisfying on thermodynamic grounds inasmuch as it relies on an expected casual relationship between the dissipation of available energy and the rise and fall of internal glucose as the system approaches equilibrium. The effects seen are implicit in the relationship, $\Delta\bar{\mu}_{Na^+} = \Delta\psi + \Delta\mu_{Na^+}$ [22]. However, experimental studies suggest that this logical explanation is too simple.

According to theory, gradient-coupled transport is bidirectional. This means that the slowing of net uptake as time progresses should be a consequence of increasing efflux due to the internal accumulation of sodium and glucose as well as of decreasing influx due to any decay in the gradients initially established. In order to verify that theory held for the brush-border membrane vesicular system, we studied the progress curves at the two extremes of glucose concentration, 20 μM and 8020 μM, with a pulsed assay to determine whether the initial rate of entry was constant or variable over time.

The data are shown in Figs. 9A and 9B where the curves represent, respectively, the cumulative net uptake of D-glucose at the time interval indicated (circles), the cumulative entry of D-glucose calculated from the sum of the measured 3-s pulses (triangles) and the internal Na^+ concentration measured with ^{22}Na (squares). The vertical bars represent the uptake for the 3-s period indicated by the width of the bars. The 3-s pulse uptakes indicate how the forward rate is responding to the forces of the gradient, which is decaying, and to the accumulation of internal sodium and D-glucose. For the purpose of quantitation and com-

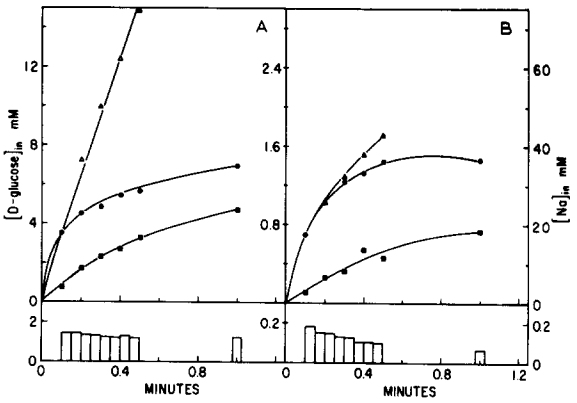

Fig. 9. Pulsed D-glucose progress curves. Vesicles were loaded with 300 mM mannitol and 5 mM Hepes-Tris (pH 7.5). The reaction was initiated by the addition of 50 μl of vesicles to a 300 μl cocktail yielding a final medium composition of 143 mM mannitol, 100 mM NaSCN, 5 mM hepes-Tris (pH 7.5), and labeled compound. The circles and squares represent the D-glucose and sodium progress curves, respectively. The concentration of D-glucose was: panel A, 8 mM containing 100 μM ^{14}C-label; and panel B, 20 μM ^{14}C-label. The bars represent the 3-s uptake concentration of D-glucose in the vesicles for the time indicated. The protocol for the bars is slightly different; the reaction was carried out as described above without labeled D-glucose to the time indicated by the left-hand side of the bar, and then the D-[^{14}C]glucose was added, and the reaction terminated 3 s later. The upper curve, triangles, represents the progressive sum of the 3-s pulses added to the measured 0.10 min D-glucose progress curve concentration. ($N = 1$).

parison of parameters the data in Fig. 9 were all collected in a single experiment carried out in duplicate on a single preparation of vesicles. They are, however, consistent with and representative of a much larger body of data in which single parameters were measured in any given experiment.

The principal features of Fig. 9 are as follows: at 8020 μM glucose (panel A) the uptake curve for glucose is typical (see Fig. 5); that is, overshoot is not seen. The 3-s pulses show a small initial decay in the entry rate followed by a nearly constant entry rate over the next 0.8 min interval, as could be expected for a reaction driven by a constant concentration of coreactant; i.e., external sodium, provided $\Delta\psi$ has no effect on the reaction or is close to $\Delta\psi = 0$ because of the decrement due to the electrogenic entry of Na^+ with glucose [22]. $\Delta\psi$; that is $\Delta\mu_{SCN}$, is certainly decaying over this time scale [21]. The constancy of the 3-s pulse uptakes strongly suggests that the curvilinear nature of cumulative uptake at 8020 μM D-glucose is a result of increasing efflux as uptake proceeds. In fact, the difference between calculated cumulative entry (triangles) and cumulative net uptake (circles) is a measure of cumulative efflux.

These observations at 8020 μM glucose accord very nicely with simple theory.

At 20 μM glucose (Panel B), on the other hand, a very different result is obtained. The 3-s pulse rate (bars) decreases with time and the calculated cumulative entry (triangles) is very nearly the same as the observed cumulative net uptake (circles). This means that efflux is so low during the first 0.5 min that the transport reaction is substantially unidirectional. Calculations (not shown) from the data between 0.4 and 0.5 min, with outward diffusion taken into account, show that carrier-mediated efflux is no more than 25% of the measured carrier-mediated influx. This result does not fit with conventional theory. If the fall in the influx rate were a consequence only of the decay of the inward gradient of Na^+ and the membrane potential (inside negative), efflux would have been expected to increase in some proportion to the outward gradient of glucose. It did not. On this basis we looked for some factor in the system, increasing with time, that could inhibit both influx and efflux when the initial external concentration of glucose was 20 μM and not when it was 8020 μM.

Internal inhibition by Na^+ and glucose

Comparison of the glucose uptake curves with the Na^+ content curves in Fig. 9 suggested the direction of further inquiry. The Na^+ content at any given time is roughly the same in panels A and B whereas the vesicular concentration of glucose is very different *. Among the possible explanations of the data, the one that seemed most plausible and also experimentally easily approachable was that internal Na^+ in the relative absence of glucose is inhibitory. If internal Na^+ and the carrier could combine to form a binary complex, $Na \cdot C$, which was not 'mobile' then the rates of influx and efflux should both be reduced as they are seen to be in Panel B. A direct test of this proposition was then made. This test is also a test of the Hopfer kinetic model because binary complex formation between internal Na^+ and the carrier is forbidden by the Hopfer model.

The results of the test are shown in Fig. 10 as the effect of Na^+ preloading of the vesicles on the glucose kinetic patterns at a fixed external $[Na^+]$ of 0.4 M with the membrane potential preset to zero as described in Materials and Methods. Internal Na^+ was varied from 0 to 60 mM producing a progressive inhibition of glucose uptake in both pathways. The inhibition is characterized by a reduction in V_{max} with no observable change in the K_m values indicating non-competitive inhibition in both pathways. The shape change in the curves with increasing internal $[Na^+]$ indicates that the pathways are inhibited to different degrees. A Dixon replot (Fig. 11) of the corrected values gives two K_i values; (30–40 mM against LAP-G and ≥ 7 mM against HAP-G. The low value of the K_i against HAP-G is in keeping with the suppression of efflux in the early time periods of Fig. 9, Panel B. On the other hand, the lack of inhibition in Fig. 9, Panel A would require that internal inhibition by Na^+ be reversible by glucose. The ability of internal glucose to prevent inhibition by internal Na^+ is shown in Fig. 12.

The test vesicles were loaded with 25 mM Na_2SO_4 and D-glucose from 0 to 16 mM. The uptakes found for the D-glucose loadings (trian-

* ^{22}Na and D-[^{14}C]glucose spaces were identical in 90-min space measurements when a large excess of the unlabeled form was added.

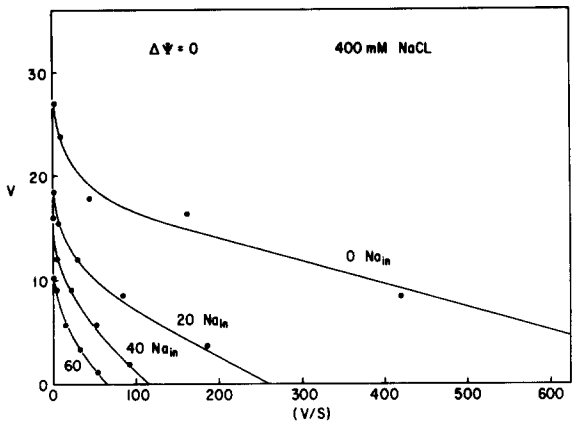

Fig. 10. The effect of sodium loading. Vesicles were loaded with 0.4 M KCl, 5 mM hepes-Tris (pH 7.5), 0.8 M mannitol less twice the NaCl loading concentration, and valinomycin. The vesicles were loaded with NaCl as follows: 0, 20 mM, 40 mM, and 60 mM. The reaction was initiated as in Fig. 1 with a final medium composition of 400 mM KCl, 400 mM NaCl, 5 mM hepes-Tris (pH 7.5), approx. 100 mM mannitol, and D-glucose at 20 μM, 100 μM, 400 μM, 2 mM, and 8 mM. The concentration of D-[^{14}C]glucose was 20 μM, and 100 μM in the other four concentrations. ($N = 1$).

gles) exceeded the sodium inhibited vesicles (open circles), and at 16 mM internal D-glucose the uptake exceeded the non-sodium loaded vesicles (closed circles). The reversal of the inhibition by

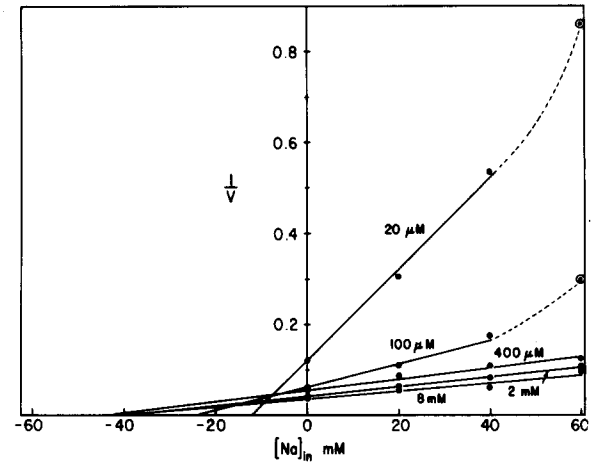

Fig. 11. Dixon plot for sodium loading. The uptake concentrations in Fig. 10 are replotted as reciprocals versus the internal concentration of sodium. Points residing on the dashed lines represent an underestimate of the velocity due to too severe an inhibition of the uptake at the earliest times of measurement.

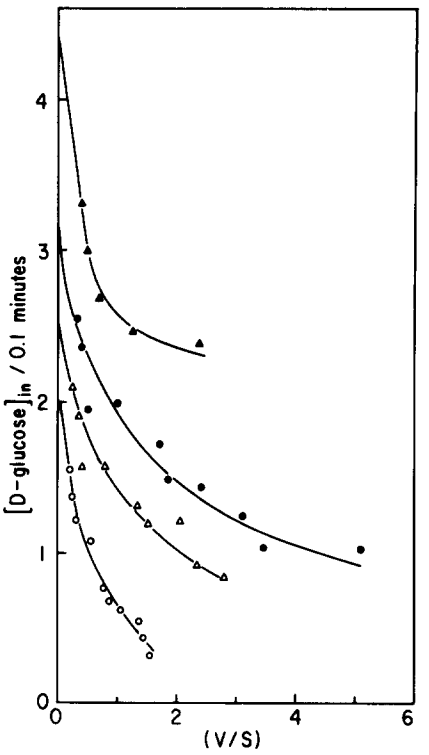

Fig. 12. Effect of products on the forward reaction. All vesicles were preloaded with 200 mM K_2SO_4, 5 mM Hepes-Tris (pH 7.5), valinomycin, mannitol for osmotic balance, and 25 mM Na_2SO_4 (except for ●). Additionally a variable D-glucose concentration was loaded: 0 (○), 4 mM (△), and 16 mM (▲). The reaction medium contained 250 mM Na_2SO_4, 200 mM K_2SO_4, 5 mM Hepes-Tris (pH 7.5), 100 μM D-[^{14}C]glucose plus a variable amount of unlabeled D-glucose up to 8 mM. ($N = 1$).

D-glucose is present in both pathways as indicated by the elevation of the V_{max} intercept.

We also tested the forward reaction for inhibition by internal D-glucose at 0.10 min under conditions of zero membrane potential. For the same technical considerations that prevented the construction of the complete kinetic patterns in Fig. 12 we only tested the general effect of high internal D-glucose (100 mM) and not the specific pathway results. Under conditions of a 400 mM NaCl gradient and high equimolar concentrations of KCl in both compartments the uptake of 2.1 mM D-glucose was inhibited by 62% ± 10%. This result is consistent with observations by Kessler and Semenza [23], and is consistent with an inhibition of both pathways.

Selective inhibition of the pathways

A modest search has been made for analogs of glucose which might show selectivity for one pathway over another. 2-Deoxy-D-glucose might be such an analog. As compared to 3-*O*-methylglucose which inhibits both pathways when present at very high concentrations, 2-deoxyglucose produces an apparently selective inhibition of HAP-G (Fig. 13). However, failure to inhibit perceptibly LAP-G could be a result of a very unfavorable K_i as with the low concentration of 3-*O*-methylglucose chosen for comparison. Unfortunately, no compound among those tested has been found to selectively inhibit LAP-G. Such a compound would have great determinative value in deciding whether the two pathways are, in fact, two separate carriers. As will be made clear in the discussion, the finding of two widely separated K_i values for inhibition by internal Na^+ (see above) is the sole experimental indication that the pathways are separate.

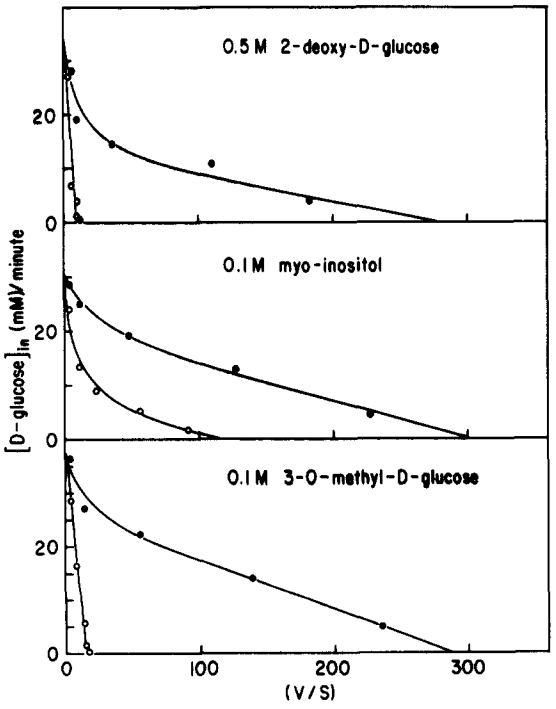

Fig. 13. Inhibition of D-glucose uptake by alternate substrates. Vesicles were loaded with 400 mM KCl, 5 mM Hepes-Tris (pH 7.5), mannitol for osmotic balance, and valinomycin. The medium contained 400 mM KCl, 5 mM Hepes-Tris (pH 7.5), 200 mM NaCl, and either mannitol (control curve) or the substrate indicated in the figure. ($N = 1$).

Correlation with the data of Hopfer and Groseclose

From the beginning of these studies correlation of our data with the data of Hopfer and Groseclose [1] has been difficult. The reason for this was that although we could confirm the existence of the same values for K_m glucose (2–5 mM) and K_i phlorizin (about 6 μM), we found these values in two different pathways, not in the same pathway. Under zero gradient conditions like those used for equilibrium exchange studies we always found a K_i for phlorizin in the high micromolar range [16]. At one point, after we knew that the Hopfer model was not correct for the transport system studied by us (see above), we attempted a rationalization on the basis of the possibility that the two groups were studying two different transport systems, only one of which was expressed fully under equilibrium exchange conditions and this one was only a minor proportion of the total activity under full gradient conditions. Personal communication from Dr. Hopfer referred us to a report on rate [24] which eliminated this possibility. The prime issue then became the K_i for phlorizin in the experiments of Hopfer and Groseclose; how it was obtained and what it means. It is clear from their paper that the decision for Na^+ add first and leave first, which is incorrect, was based entirely upon the results with phlorizin. Personal communication with Dr. Hopfer further revealed that the experiment with phlorizin was actually done by glucose uptake rather than by equilibrium exchange as had been our impression from the information available in the paper. This meant that both groups had been using what appeared to be the identical method but had obtained very different results. Was there a critical step in the methodology? Comparison of the methods used by Hopfer and Groseclose with our own disclosed that the sole difference seemed to be the means used to load vesicles with the external salt solution.

We decided to repeat the measurements with vesicles prepared by both methods and to compare the results. These are shown in Fig. 14. Using our method for preparing loaded vesicles gave a result (about 80 μM) which is somewhat lower but consistent with the value (about 120 μM for LAP-G) calculated from computer resolved plots obtained under gradient conditions. The equilibration method of Hopfer; that is, incubation of mannitol

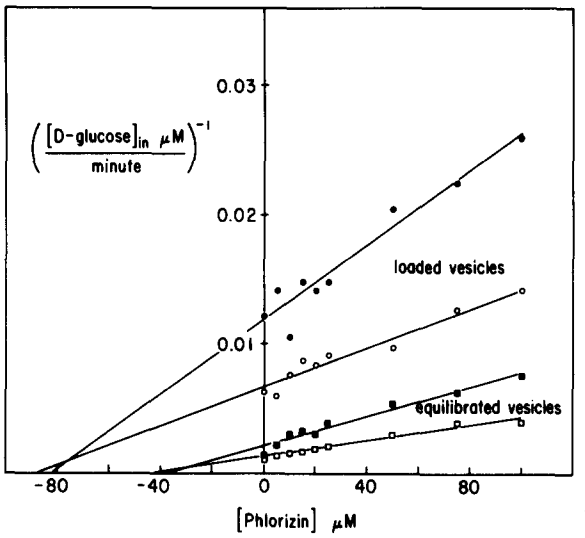

Fig. 14. Phlorizin inhibition in sodium-equilibrated vesicles. Vesicles were prepared as described in Methods, the loaded and equilibrated designations used here refer to the method of preparation. Loaded vesicles (circles) are those suspended in NaSCN after the first high-speed spin, and equilibrated vesicles (squares) are those suspended in mannitol at that point. Closed symbols represent 50 μM D-[^{14}C]glucose in the reaction medium, and open symbols represent 100 μM D-[^{14}C]glucose ($N = 1$).

loaded vesicles for 30 min at room temperature, gave a substantially lower value (about 30 μM). If the vesicles were not equilibrated we would expect a value of about 13 μM based upon the estimated contributions of the two pathways at the concentrations of glucose selected. The experiments of Fig. 14 were carried out at 15°C. A value of 6 μM would be expected to be seen at a temperature of about 20°C based upon our observations (not shown) of the effect of temperature on K_i phlorizin.

From a theoretical, and we believe a demonstrated practical, point of view our procedure for obtaining equilibrated vesicles by directly forming them in a solution identical to the incubation medium is superior to methods which depend upon an unmonitored exchange of internal and external solution during an arbitrarily chosen time period of incubation. Consistent with this opinion, the points of intersection with the ordinate show a slower V_{max} for the vesicles prepared by our method as would be expected for a higher internal Na^+ content with its inhibitory effect on transport.

Discussion

In this paper we have described two readily distinguishable kinetic pathways, LAP-G and HAP-G, for the Na^+-dependent transport of D-glucose into vesicles prepared from rabbit jejunal brush-border membranes. The two pathways described herein resemble the two pathways described for intact rat intestine, in vitro, by Lyon and Crane [3]. In both cases there is a high-affinity and a low-affinity pathway with relative constants for glucose and Na^+ that are approximately in the same proportion. The absolute values for the constants differ substantially, the values of Lyon and Crane for glucose being much the higher, but this difference may be attributed to the 'unstirred layer' effect in intact intestine [25]. At least one of the pathways described herein is not the same as one of the two pathways described by Honegger and Semenza [4] in hamster intestine. One of the pathways in hamster intestine is distinguished by its inability to use 3-*O*-methylglucose as a substrate. Both pathways studied by us utilize 3-*O*-methylglucose. The measured kinetic properties of our two pathways are not the same as those of the two pathways recently described in rabbit kidney, the signal difference being the K_i of phlorizin relative to the K_m for glucose. In the kidney, the low-affinity pathway for glucose has a high affinity for phlorizin and the other way around in the other pathway [26]. 3-*O*-Methylglucose is also not a substrate for the low-affinity pathway of the kidney.

In carrying out these studies we have attempted to take into account all of the objections known to us of kinetic studies of transport systems carried out with membrane vesicles. We have shown that the morphology of the vesicles does not account for their apparent kinetics. There is a single population of vesicles with a mean diameter of 135 nm and varying degrees of contamination by other forms does not alter the kinetic patterns. If there are two functionally distinct kinds of brush-border membrane to account for the two pathways, they are not readily separable as are the two kinds of vesicles, outer cortical and outer medullary, recoverable from kidney [26]. We have studied the system with and without Na^+ gradients, with and without a membrane potential. LAP-G is always

seen. HAP-G is sometimes not seen, as when the Na^+ electrochemical gradient is set at zero. However, HAP-G does not require a membrane potential in order to be expressed. Increasing the external [Na^+] in the absence of a membrane potential reveals HAP-G to a major fraction of the rate achieved by the further addition of a membrane potential [16].

We have corrected the data collected at real times to time zero by a mathematical procedure accepted for enzymes [12] and we know of no objection to the use of this procedure for a transport system. Moreover, correction of the data changes nothing grossly. The values assigned to the kinetic constants change somewhat but not to a degree that would alter any conclusions.

Until the completion of the studies on the inhibitory effects of internal Na^+, we strongly favored an interpretation of the two pathways for Na^+-dependent glucose influx as the two external legs of a random bi-bi steady-state kinetic model [27,28]. This model, which is among the most complex models considered by Segel [29], accommodates a number of our observations that have, so far as we can see, no other easy or, at least, anticipated explanation. For example, this model sets a thermodynamic requirement for the relationship of the K_d values of the two substrates in the two pathways which is approached by the K_m values we have obtained. Labelling the pathways, respectively, $K_1 + K_2$ and $K_3 + K_4$, then the relationship must hold that $K_1 \cdot K_2 = K_3 \cdot K_4$ [29]. The relationship we find, using the data from Table III for glucose and from a previous publication [16] for Na^+, is $K_1 \cdot K_2 = 32.8$ and $K_3 \cdot K_4 = 7.4$ with overlap at 12; i.e., at 1 standard deviation. Also, in studies described earlier [16], we applied increasing gradients of Na^+ and membrane potential to find that a total maximal rate of about 18 pmol/0.25 min per mg was not exceeded no matter how steep the gradient and the shape of the Hofstee plot changed as though by the reproportionation of pathway activity predicted by the random bi-bi steady-state model [29]. When the inhibitory effect of internal Na^+ was found we revised the model to random bi-ordered bi [16]. When the inhibitory effect was found to have a different K_i against the two influx pathways (Fig. 10) we felt obliged to abandon the concept of a single transporter.

The stoichiometry of Na^+-dependent glucose transport by rabbit jejunal brush-border membrane vesicles has been estimated by Hopfer and Groseclose to be 1 : 1 and by Kaunitz et al. [30,31] to be 2 : 1 (Na^+/glucose). Our own estimates from data such as the difference in Na^+ uptake in Fig. 9, A and B, are more than 1 : 1 and less than 2 : 1. If we consider that two pathways are involved all these estimates may be correct. LAP-G, which Hopfer effectively isolates under zero-gradient conditions, could have a stoichiometry of 1 : 1 and HAP-G, a stoichiometry of 2 : 1. This would match the stoichiometries reported for the separated low- and high-affinity transporters of the kidney [26] and give some added weight to the concept of two distinct transport systems in the rabbit intestine. On the other hand, the varying stoichiometries may only indicate a complexity in the mechanism of transport for which a kinetic model has not yet been visualized.

If one compares, point by point to the extent that data exist in the literature, the kinetic parameters of Na^+-dependent glucose transport in the intestine and the kidney one may be struck by the fact that there is no concordance of the data strict enough to support an identification of one transport system with another. Two Na^+-dependent glucose transport systems have been physically separated from the kidney. Our present position is that there are two transport systems in rabbit intestine. The differences in measured parameters between the two kidney and two intestinal systems are not subtle and, until it may be shown that these differences are based in methodology, the kidney and intestinal carriers may be assumed to lack identity.

The importance of studies of these systems which rely not at all on theory or expectation from analogy may be pointed up by the unexpected nature of the overshoot with its apparent basis in inhibition by internal Na^+ shown in Fig. 9B. The use of a difference in overshoot as, for example, by Barrett and Aronson [32] to prove an alteration in available energy must be shown not to have a different, less obvious basis.

Acknowledgments

This work was supported by a grant from NIAMDD. We are indebted to Dr. Bijan Ghosh for the data on vesicle population shown in Fig. 1. We are also indebted to Dr. G. Semenza for a prepublication copy of Kessler and Semenza [23] and to Drs. E.M. Wright and J.D. Kaunitz for a copy of an as yet unpublished manuscript in which two pathways for Na^+-dependent glucose transport in rabbit jejunal brush-border membrane vesicles are shown.

References

1 Hopfer, U. and Groseclose, R. (1980) J. Biol. Chem. 255, 4453–4462
2 Turner, R.J. and Silverman, M. (1981) J. Membrane Biol. 58, 43–55
3 Lyon, I. and Crane, R.K. (1966) Biochim. Biophys. Acta 112, 278–291
4 Honegger, P. and Semenza, G. (1973) Biochim. Biophys. Acta 318, 390–410
5 Malathi, P., Preiser, H., Fairclough, P., Mallett, P. and Crane, R.K. (1979) Biochim. Biophys. Acta 554, 259–263
6 Hopfer, U. (1977) J. Supramol. Struct. 7, 1–13
7 Hopfer, U. (1977) Am. J. Physiol. 233, E445–449
8 Hopfer, U. (1978) Am. J. Physiol. 234, F89–F96
9 Hopfer, U. (1981) Fed. Proc. 40, 2480–2485
10 Pressman, B.C. (1968) Fed. Proc. 27, 1283–1288
11 Lowry, O.H., Rosebrough, N.J., Farr, A.L. and Randall, R.J. (1951) J. Biol. Chem 193, 265–275
12 Cornish-Bowden, A. (1976) in Principles of Enzyme Kinetics. (ed.) pp. 142–193, Butterworths, London
13 Kinne, R., Murer, H., Kinne-Saffran, E., Thees, M. and Sachs, G. (1975) J. Membrane Biol. 21, 275–295
14 Caspary, W.F. and Crane, R.K. (1968) Biochim. Biophys. Acta 163, 395–400
15 Toggenburger, G., Kessler, M., Rothstein, A., Semenza, G. and Tannenbaum, C. (1978) J. Membrane Biol. 40, 269–290
16 Crane, R.K. and Dorando, F.C. (1982) in Membranes and Transport, Vol. 2 (Martonosi, A., ed.), pp. 153–160, Plenum Press Corporation, New York
17 Toggenburger, G., Kessler, M. and Semenza, G. (1982) Biochim. Biophys. Acta 688, 557–571
18 Kessler, M., Tannenbaum, V. and Tannenbaum, C. (1978) Biochim. Biophys. Acta 509, 348–359
19 Hopfer, U., Nelson, K., Perrotto, J. and Isselbacher, K.J. (1973) J. Biol. Chem. 248, 25–32
20 Murer, H. and Hopfer, U. (1974) Proc. Natl. Acad. Sci. U.S.A. 71, 484–488
21 Kessler, M. and Semenza, G. (1979) FEBS Lett. 108, 205–208
22 Crane, R.K. (1977) Rev. Physiol. Biochem. Pharmacol. 78, 99–159
23 Kessler, M. and Semenza, G. (1983) J. Membrane Biol. 76, 27–56
24 Hopfer, U. and Prevencher, S.W. (1982) Biophys. J. 37, 339a
25 Wilson, F.A. and Dietschy, J.M. (1974) Biochim. Biophys. Acta 363, 112–126
26 Turner, R.J. and Moran, A. (1982) Am. J. Physiol. 242, F406–F414
27 Crane, R.K. and Dorando, F.C. (1979) in Function and Molecular Aspects of Biomembrane Transport (Quagliariello, E., Palmieri, F., Papa, S. and Klingenberg, M., eds.), pp. 271–277, Elsevier/North-Holland, Amsterdam
28 Crane, R.K. and Dorando, F.C. (1980) Ann. N.Y. Acad. Sci. 339, 46–52
29 Segel, I.H. (1975) Enzyme Kinetics, pp. 957, Wiley-Interscience, New York
30 Kaunitz, J.D. and Wright, E.M. (1983) Fed. Proc. 42, 1287
31 Kaunitz, J.D., Gunther, R. and Wright, E.M. (1982) Proc. Natl. Acad. Sci. U.S.A. 79, 2315–2318
32 Barrett, P.Q. and Aronson, P.S. (1983) Am. J. Physiol. 242, F126–F131